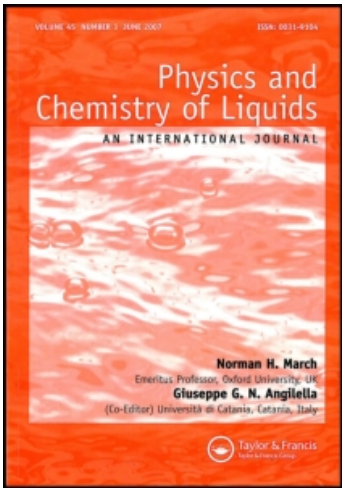

Physics and Chemistry of Liquids
Publication details, including instructions for authors and subscription information:
http://www.informaworld.com/smpp/title~content=t713646857

Phase diagrams of ascending and minimum type in terms of concentration fluctuations in binary liquid and solid solutions

A. B. Bhatia[a]; N. H. March[ab]
[a] Department of Physics, University of Alberta, Edmonton, Canada [b] Department of Physics, Imperial College, South Kensington, London, England

To cite this Article Bhatia, A. B. and March, N. H.(1976) 'Phase diagrams of ascending and minimum type in terms of concentration fluctuations in binary liquid and solid solutions', Physics and Chemistry of Liquids, 5: 1, 45 — 60
To link to this Article: DOI: 10.1080/00319107608084106
URL: http://dx.doi.org/10.1080/00319107608084106

Phys. Chem. Liq., 1976, pp. 45–60

Printed in Dordrecht, Holland

Phase Diagrams of Ascending and Minimum Type in Terms of Concentration Fluctuations in Binary Liquid and Solid Solutions†

A. B. BHATIA
Department of Physics, University of Alberta, Edmonton, Canada

and

N. H. MARCH‡

The thermodynamics of binary alloy phase diagrams of ascending and minimum types is shown to lead to a rather direct relation between the ratio of the slopes of the liquidus and the solidus curves, at a given temperature T, and the ratio $\langle(\Delta c)^2\rangle^l/\langle(\Delta c)^2\rangle^s$ of the concentration fluctuations in the liquid and the solid solutions. The latent heats of the two pure components also enter in a direct manner, as could have been anticipated from the results of ideal solution theory.

Minimum type phase diagrams are not possible in ideal solutions nor in conformal solutions with the same interaction energies in solid and liquid states. But they are shown to arise naturally in our formalism from differences in behaviour of $\langle(\Delta c)^2\rangle^l$ and $\langle(\Delta c)^2\rangle^s$.

Application has then been made to four alloy systems, Ag – Au, Cd – Mg, Bi – Sb having ascending type phase diagrams, and Au – Cu of the minimum type. In Cd – Mg and Au – Cu, the conformal solution model works well, with physically reasonable choices of the interaction energies ω_l and ω_s in liquid and solid. In minimum type solutions, the minimum temperature and corresponding concentration are shown to depend only on the difference $\omega_l - \omega_s$. For Ag–Au and Bi–Sb, there is no difficulty in getting the shapes of liquidus and solidus curves correctly from the conformal solution model, although there are some discrepancies of detail. Finally, some brief comments are made about the concentration fluctuations in Au – Pt alloys from the known phase diagram.

---

†Work supported in part by the National Research Council of Canada.

‡Present address: *Department of Physics, Imperial College, South Kensington, London S.W.7, England.* The contribution of one of us (NHM) to this work was largely carried out during a visit to the Physics Department, University of Alberta, Edmonton in the summer of 1974.

1 INTRODUCTION

Listed in Hansen[4] are numerous examples of binary alloy phase diagrams of ascending and of minimum type. Figure 1 shows schematically (i–iv) examples of diagrams of ascending type, and also (v) the minimum type of liquidus and solidus behaviour.

While some attention has been paid hitherto to the calculation of individual diagrams (see, for example, Reisman[8] and other references given there), our aim in present work is rather different. We want to combine recent progress in our understanding of concentration fluctuations in solutions with a more careful thermodynamical discussion of the two qualitatively different types of diagrams shown in Figure 1. When *ideal* solution theory is applied, different characteristics of the ascending type diagrams have been shown[8] to arise from variations in the melting temperatures and latent heats of the pure components A and B. But when we study even such a relatively simple alloy system as Ag–Au, quantitative agreement cannot be obtained in this way. But more important for our present discussion, ideal solution theory *cannot* lead to the minimum type of phase diagram (Fig. 1 v).

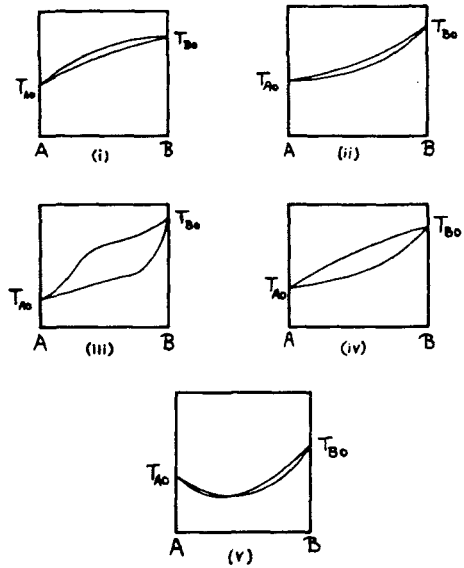

FIGURE 1 Schematic forms of phase diagrams of ascending and minimum type: (i) Phase diagram showing both liquidus and solidus to be concave, e.g. A = Ag, B = Au. (ii) Phase diagram showing both liquidus and solidus to be convex, e.g. A = Cd, B = Mg. (iii) Phase diagram showing inflected curves for liquidus and solidus, e.g. A = Au, B = Pt. (iv) Phase diagram with liquidus convex and solidus concave, e.g. A = Cu, B = Ni. (v) Minimum type phase diagram, e.g. A = Rb, B = K.

We have already calculated[1,2] the liquidus curves of some simple eutectic binary alloys (a) from conformal solution theory[6] and (b) from a theory of the Flory (1942) type, which can incorporate large size differences between the components. One result[1] which turns out to be directly useful in interpreting the shapes of liquidus curves in such eutectics is the formula for the slope $\Delta T/\Delta C_2$, given by

$$\frac{\Delta T}{\Delta c_2} = -\frac{RT^2 c_2}{S_{CC} L}. \tag{1.1}$$

Here $c_2 = 1 - c$, c being the concentration of component 1, while S_{CC}, of course, in a eutectic, refers to the concentration fluctuations in the liquid solution and is defined precisely by

$$S_{CC} = N\langle(\Delta c)^2\rangle = Nk_B T/\left(\frac{\partial^2 G_m}{\partial c^2}\right)_{T,P,N}, \tag{1.2}$$

G_m being the Gibbs free energy of mixing. L in (1.1) is a generalized concentration-dependent latent heat defined by the writers[1] and in lowest order $L \simeq L_{10}$, the latent heat of pure component 1.

It is perfectly clear qualitatively that the new feature which must enter the theory when we turn from eutectics to the phase diagrams shown in Figure 1 is a description of the concentration fluctuations $\langle(\Delta c)^2\rangle^s$ in the solid solution. One simplification that it is important to emphasize in this connection is that, (see Figure 1), we are dealing in the present paper with alloys which form continuous solid solutions. These are characterized by relatively *small* size differences and generally the solid pure elements A and B have the same crystal structure.

One of the main findings of the present work (see Section 3.1 below) is that the equilibrium conditions (Section 2) for the phase diagrams shown in Figure 1 yield generalizations of the formula (1.1) for the slopes of the liquidus and solidus curves. In view of our remarks in the previous paragraph, it should occasion no surprise that the slope of the solidus involves directly the concentration fluctuations $\langle(\Delta c)^2\rangle^s$ in the solid solution (Eq. 3.11 below). Naturally, our equations reduce to the well-known forms[8] (also Section 5 below) for ideal solutions. For the calculations of specific phase diagrams, we shall use here the model of conformal solutions† (see sections 6 and 7).

†A necessary, though not sufficient, condition for this model to apply is that size differences are not too large. This, we have already noted, is the case for the diagrams of Figure 1.

2 THERMODYNAMIC EQUATIONS

As used above, the superscripts l and s refer respectively to the liquid and solid solution. N_A^l and N_B^l refer to the numbers of the two types of atoms in the liquid. An additional subscript O will indicate the appropriate pure component.

We shall work with liquid (c_l) and solid (c_s) concentrations given by

$$c_l \equiv N_B^l/(N_A^l + N_B^l) \tag{2.1}$$

and

$$c_s = N_B^s/(N_A^s + N_B^s). \tag{2.2}$$

If the chemical potentials of A(B) in liquid and solid solutions are denoted by μ_A^l, μ_A^s, μ_B^l and μ_B^s, then the equilibrium conditions are given by

$$\mu_A^l = \mu_A^s \tag{2.3}$$

and

$$\mu_B^l = \mu_B^s \tag{2.4}$$

Here, of course, the μ's are functions of T and P and of c_l or c_s.

2.1 Equilibrium conditions in terms of activities

It will be helpful at this point to express the equilibrium conditions (2.3) and (2.4) in terms of activities a. These are defined by

$$\mu_A^l = \mu_{AO}^l + RT \ln a_A^l = \mu_{AO}^l + RT \ln \gamma_A^l (1-c_l) \tag{2.5}$$

$$\mu_A^s = \mu_{AO}^s + RT \ln a_A^s = \mu_{AO}^s + RT \ln \gamma_A^s (1-c_s) \tag{2.6}$$

$$\mu_B^l = \mu_{BO}^l + RT \ln a_B^l = \mu_{BO}^s + RT \ln \gamma_B^l c_l \tag{2.7}$$

and

$$\mu_B^s = \mu_{BO}^s + RT \ln a_B^s = \mu_{BO}^s + RT \ln \gamma_B^s c_s. \tag{2.8}$$

The activity coefficients γ have also been introduced in Eqs. (2.5–2.8); in terms of these an ideal solution is characterized by all γ's equal to unity.

Using the Eqs. (2.3–2.8), we can write the conditions for equilibrium in the forms

$$\frac{\gamma_A^l(1 - c_l)}{\gamma_A^s(1 - c_s)} = \exp(-F_{AO}/RT), \tag{2.9}$$

and

$$\frac{\gamma_B c_l}{\gamma_B^s c_s} = \exp(-F_{BO}/RT), \tag{2.10}$$

where the quantities F_{AO} and F_{BO} are solely properties of the pure components and are defined by

$$F_{AO} = \mu^{l}_{AO} - \mu^{s}_{AO} \tag{2.11}$$

and

$$F_{BO} = \mu^{l}_{BO} - \mu^{s}_{BO}. \tag{2.12}$$

It is clear then that if we have knowledge of the thermodynamics of the pure components A and B, plus information about the solutions (both liquid and solid) summarized in the activities, then Eqs. (2.9) and (2.10) can be solved simultaneously to yield the liquidus $c_l(T)$ and the solidus $c_s(T)$. Before turning to discuss the results of Eqs. (2.9) and (2.10) for simple models, we take up the point raised in the Introduction, namely the generalizations of (1.1) appropriate to the liquidus and solidus curves.

3 SLOPES OF LIQUIDUS AND SOLIDUS CURVES

To obtain expressions for the slopes of the liquidus $(\Delta T/\Delta c_l)$ and of the solidus curves $(\Delta T/\Delta c_s)$, we can obviously write from the equilibrium conditions $\mu^{l}_{A}(T, c_l) = \mu^{s}_{A}(T, c_s)$

$$\mu^{l}_{A}(T + \Delta T, c_l + \Delta c_l) = \mu^{s}_{A}(T + \Delta T, c_s + \Delta c_s) \tag{3.1}$$

and hence it follows, using Eqs. (2.5–2.8) that

$$\Delta T\left[\frac{\partial}{\partial T}\mu^{l}_{AO} + \left(\frac{\partial}{\partial T}[RT \ln a^{l}_{A}]\right)_{c_l}\right] + \left(\frac{\partial}{\partial c_l}[RT \ln a^{l}_{A}]\right)_{T} \Delta c_l =$$

$$\Delta T\left[\frac{\partial}{\partial T}\mu^{s}_{AO} + \left(\frac{\partial}{\partial T}[RT \ln a^{s}_{A}]\right)_{c_s}\right] + \left(\frac{\partial}{\partial c_s}[RT \ln a^{s}_{A}]\right) \Delta c_s. \tag{3.2}$$

Following our earlier work (Bhatia and March 1972) on eutectic systems, we now introduce a generalized concentration-dependent latent heat L_A of A through

$$\frac{L_A}{T} = \frac{\partial}{\partial T}(\mu^{s}_{AO} - \mu^{l}_{AO}) - \frac{\partial}{\partial T}(RT \ln a^{l}_{A}/a^{s}_{A}). \tag{3.3}$$

We note that as $c_l, c_s \to O$, $L_A \to L_{AO}$. Using (3.3) in (3.2), we have

$$\frac{L_A}{RT^2}\Delta T = \frac{\partial \ln a^{l}_{A}}{\partial c_l}\Delta c_l - \frac{\partial \ln a^{s}_{A}}{\partial c_s}\Delta c_s. \tag{3.4}$$

Similarly from the second equilibrium equation we obtain

$$\frac{L_B}{RT^2}\Delta T = \frac{\partial \ln a_B^l}{\partial c_l}\Delta c_l - \frac{\partial \ln a_B^s}{\partial c_s}\Delta c_s. \tag{3.5}$$

3.1 Introduction of concentration fluctuations

Evidently from Eq. (1.2) the concentration fluctuations S_{CC}† can be related to the activities. The results are

$$\frac{d \ln a_B^l}{dc_l} = \frac{1 - c_l}{S_{CC}^l}; \quad \frac{d \ln a_B^s}{dc_s} = \frac{1 - c_s}{S_{CC}^s} \tag{3.6}$$

and

$$\frac{d \ln a_A^l}{dc_l} = -\frac{c_l}{S_{CC}^l}; \quad \frac{d \ln a_A^s}{dc_s} = -\frac{c_s}{S_{CC}^s}. \tag{3.7}$$

Equations (3.4) and (3.5) then take the form

$$\frac{L_A}{RT^2}\Delta T = -\frac{c_l}{S_{CC}^l}\Delta c_l + \frac{c_s}{S_{CC}^s}\Delta c_s \tag{3.8}$$

and

$$\frac{L_B}{RT^2}\Delta T = \frac{1 - c_l}{S_{CC}^l}\Delta c_l - \frac{(1 - c_s)}{S_{CC}^s}\Delta c_s. \tag{3.9}$$

Eliminating first Δc_s between (3.8) and (3.9), the slope of the liquidus is found as‡

$$\frac{\Delta T}{\Delta c_l} = -\frac{RT^2(c_l - c_s)}{S_{CC}^l\left[L_A(1 - c_s) + L_B c_s\right]}. \tag{3.10}$$

This equation is the required generalization of the result (1.1) for the liquidus of a eutectic alloy. Similarly by eliminating Δc_l between (3.8) and (3.9) we find

$$\frac{\Delta T}{\Delta c_s} = -\frac{RT^2(c_l - c_s)}{S_{CC}^s\left[L_A(1 - c_l) + L_B c_l\right]}. \tag{3.11}$$

---

† In the solid, S_{CC}^s denotes $\langle(\Delta c)^2\rangle^s$ and is *not* the $q \to 0$ limit of the structure factor. Such a difference does not exist in the liquid.[3]

‡ It will be evident that equations of the type (3.10–3.12) are applicable not only to equilibrium between the liquid and solid alloy but equally to equilibrium between any pair of phases of a binary system, with appropriate interpretation of the suffixes l and s and the latent heats. Their essential content has been known and used in different contexts since the time of Gibbs and Konowalow, see, for example, Rowlinson.[] They do not seem to have occurred in the literature in the present form (using S_{CC}), and, as far as we are aware, have not been previously applied to the study of the slopes of the liquidus and solidus.

Hence at a given temperature, the ratio of the slopes of liquidus to solidus curves is given by

$$\frac{\Delta T}{\Delta c_l}\Big/\frac{\Delta T}{\Delta c_s} = \frac{S^s_{CC}\left[L_A(1 - c_l) + L_B c_l\right]}{S^l_{CC}\left[L_A(1 - c_s) + L_B c_s\right]}. \tag{3.12}$$

This formula demonstrates that if we draw tangents to liquidus and solidus curves at a given temperature T, the ratio of the slopes involves in a direct way the ratio of the concentration fluctuations in the liquid solution and in the solid solution.

Equations (2.9) and (2.10), together with the slopes of liquidus and solidus curves in equations (3.10) and (3.11) are then the fundamental equations determining the phase diagrams of the alloy systems with which we are concerned here.

4 APPROXIMATE TREATMENT OF PURE COMPONENTS IN TERMS OF LATENT AND SPECIFIC HEATS

So far our formalism is a consequence of thermodynamics and therefore is exact. However, in using Eqs. (2.9) and (2.10) in practical calculations, it is very helpful to express F_{AO} and F_{BO}, the differences in chemical potentials in liquid and solid (see Eqs. (2.11) and (2.12)) in terms of the latent and specific heats of the pure components. Let T_{AO} be the melting temperature of pure A component. Then we can write

$$\begin{aligned} F_{AO} &= \mu^l_{AO}(T) - \mu^s_{AO}(T) \\ &= \mu^l_{AO}(T_{AO}) - \mu^s_{AO}(T_{AO}) + \int_{T_{AO}}^{T} dT' \left[\left(\frac{\partial \mu^l_{AO}}{\partial T} - \frac{\partial \mu^s_{AO}}{\partial T} \right)_{T=T_{AO}} \right. \\ &\quad \left. + \int_{T_{AO}}^{T'} dT'' \left(\frac{\partial^2 \mu^l_{AO}}{\partial T^2} - \frac{\partial^2 \mu^s_{AO}}{\partial T^2} \right)_{T=T''} \right] \end{aligned} \tag{4.1}$$

The first two terms together in (4.1) are zero from the equilibrium condition. We have also

$$\left[\frac{\partial \mu^l_{AO}}{\partial T} - \frac{\partial \mu^s_{AO}}{\partial T} \right]_{T=T_{AO}} = S^s_{AO} - S^l_{AO} = -\frac{L_{AO}}{T_{AO}}. \tag{4.2}$$

Furthermore

$$\left[\frac{\partial^2 \mu^l_{AO}}{\partial T^2} - \frac{\partial^2 \mu^s_{AO}}{\partial T^2} \right] = \frac{c^s_{pAO} - c^l_{pAO}}{T} \equiv -\frac{\Delta_{AO}}{T}, \tag{4.3}$$

i.e. the second derivatives are given by the specific heat differences. Hence we can write

$$F_{AO} = L_{AO}\left(1 - \frac{T}{T_{AO}}\right) - \int_{T_{AO}}^{T} dT' \left(\int_{T_{AO}}^{T'} \frac{\Delta_{AO}}{T''} dT''\right) \tag{4.4}$$

and

$$F_{BO} = L_{BO}\left(1 - \frac{T}{T_{BO}}\right) - \int_{T_{BO}}^{T} dT' \left(\int_{T_{BO}}^{T'} \frac{\Delta_{BO}}{T''} dT''\right) \tag{4.5}$$

Our earlier work[2] indicates that usually the term in Δ in (4.4) or (4.5) is a small correction and in the practical evaluations reported below we shall therefore neglect it.

To be definite, we shall always choose, throughout the paper, the element A to have the lower melting point, i.e. $T_{AO} < T_{BO}$.

5 PHASE BOUNDARIES FOR IDEAL AND CONFORMAL SOLUTIONS

We shall next consider the consequences of the treatment embodied in Eqs. (2.9) and (2.10) for two simple models.

5.1 Ideal solutions

Here $\gamma_A^l = \gamma_A^s = 1$, and if we write (neglecting Δ in Eqs. (4.4) and (4.5))

$$\exp\left(-\frac{F_{AO}}{RT}\right) = \exp\left[-\frac{L_{AO}}{RT}\left\{1 - \frac{T}{T_{AO}}\right\}\right] = A(T) \tag{5.1}$$

and similarly

$$\exp\left(-\frac{F_{BO}}{RT}\right) = \exp\left[-\frac{L_{BO}}{RT}\left\{1 - \frac{T}{T_{BO}}\right\}\right] = B(T) \tag{5.2}$$

then

$$1 - c_l = (1 - c_s)A \tag{5.3}$$

and

$$c_l = c_s B.$$

The solution for the liquidus is evidently

$$c_l = \frac{B(A - 1)}{A - B} \tag{5.4}$$

and for the solidus

$$c_s = \frac{(A - 1)}{(A - B)} \tag{5.5}$$

These are well known results[8] and show that c_l and c_s depend on the latent heats and melting temperatures of the pure components. While these equations reveal some of the qualitative features of ascending phase diagrams (but not of minimum type, see the Appendix), they must be transcended to describe metallic alloys by inclusion of departures from ideality.

5.2 Conformal solutions

The simplest inclusion of some degree of non-ideality (basically, weak interaction) can be made via the zeroth regular (or a little more generally, conformal) solution approximation. Here, if the interaction energies in the liquid and solid solutions respectively are ω_l and ω_s, the activity coefficients take the form

$$\ln \gamma_A^l = \frac{\omega_l c_l^2}{RT}, \quad \ln \gamma_B^l = \frac{\omega_l (1 - c_l)^2}{RT} \tag{5.6}$$

$$\ln \gamma_A^s = \frac{\omega_s c_s^2}{RT}, \quad \ln \gamma_B^s = \frac{\omega_s (1 - c_s)^2}{RT}. \tag{5.7}$$

Inserting these results into Eqs. (2.9) and (2.10), and using Eqs. (4.4) and (4.5), the two equilibrium equations can be solved simultaneously by numerical methods for $c_l(T)$ and $c_s(T)$, the input data being the known latent heats and melting temperatures of the pure components A and B, and the two interaction energies ω_l and ω_s.

Though we recognize that this is an oversimplified model for numerous ascending and minimum type phase diagrams, it will be useful to begin the discussion by taking a specific example, Ag–Au, and working out the way the shapes of the liquidus and solidus curves depend on the interaction parameters.

6 PHASE DIAGRAM FOR Ag–Au FROM CONFORMAL SOLUTION MODEL

For Ag–Au we have as input data (A = Ag)

$$T_{AO} = 1234°K, \qquad T_{BO} = 1336°K$$

$$L_{AO}\,(\text{cal/mole}) = 2690, \quad L_{BO}\,(\text{cal/mole}) = 3050.$$

As the simplest starting assumption we will take $\omega_l = \omega_s = \omega$, say, and consider how the choice of ω affects the ideal curves. We have plotted in Figure 2 the results for the choice $\omega_l = \omega_s = 2120°K$, † and the two crosses at

† This value was estimated from heat of mixing data.[5]

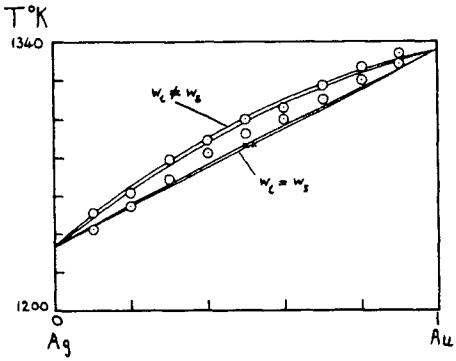

FIGURE 2 Liquidus and solidus curves for Ag–Au. The crosses denote points from "ideal" solution theory, around c ~ 0.5. The interaction with $\omega_l = \omega_s$ contracts the ideal curves slightly in this case. ⊙ Experimental points taken from Hansen.[4] Curves marked $\omega_l \neq \omega_s$ are from conformal solution theory.

$c \sim 0.5$ show that the ideal curves $\omega_l = \omega_s = 0$ are slightly narrowed by interactions of this magnitude, but that the influence of such interaction energies on the ideal curves is very small in this case. At $c_l = 0.5$, $[c_s - c_l]_{ideal} = 0.022$ whereas $c_s - c_l = 0.012$ with the interaction energies shown. The observed curves are also shown, they lie above these calculated curves and have a substantially greater separation between solidus and liquidus. However, changing ω_s slightly to -2185°K yields the curves marked $\omega_l \neq \omega_s$ in Figure 2. The concavity of the liquidus and solidus curves is then correctly given, though the width between them is too small to agree with experiment.

7 OTHER ALLOY SYSTEMS WITH ASCENDING TYPE PHASE DIAGRAMS

Because they have qualitatively different features from Ag–Au, we shall consider also the further systems

	T_{AO}°K	T_{BO}	L_{AO}(cal/mole)	L_{BO}
(i) Cd–Mg	594	922	1530	2100
and				
(ii) Bi–Sb	544°K	903°K	2600	4700

For Cd–Mg we estimated from heat of mixing data that $w \sim -3000$°K. As Figure 3 shows, we do not get agreement with experiment if we take $\omega_l = \omega_s = -3000$°K. We have therefore made ω_s less negative, and the results $\omega_s = -2735$°K are also shown in Figure 3. These are in quite satisfactory agreement with experiment.

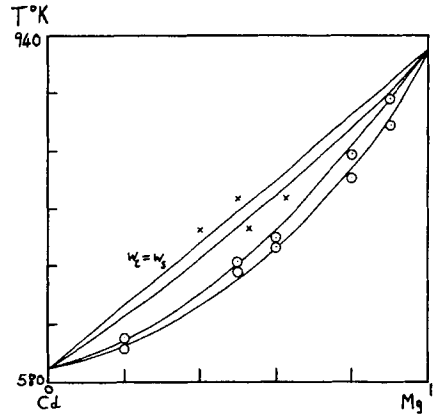

FIGURE 3 Liquidus and solidus curves for Cd–Mg. The crosses denote "ideal" solution values. Upper pair of curves from conformal solution theory with $\omega_l = \omega_s$; lower pair for $\omega_l \neq \omega_s$. ⊙ Experimental points taken from Hansen.[4]

Finally, for the ascending types of diagram, we have considered the system Bi–Sb. The ideal curves (dashed) and Hansen's curves are shown in Figure 4. If ω_l and ω_s are assumed to be independent of temperature, then the heat of mixing data[5] implies $\omega_l = 600°\,\mathrm{K}$ and $\omega_s = 0 \pm 400°\,\mathrm{K}$. This does not give the correct trends from the ideal solution curves. We have determined ω_l and ω_s from the observed values of c_s and T when $c_l = \frac{1}{2}$, obtaining $\omega_l = 121°\mathrm{K}$ and $\omega_s = 756°\,\mathrm{K}$. The dashed curves with crosses are calculated taking these values for ω_l and ω_s. While the agreement with experiment is good, there

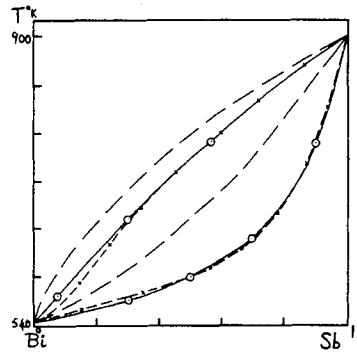

FIGURE 4 Liquidus and solidus curves for Bi–Sb (example of type (iv) of Figure 1). Ideal curves (dashed lines); experimental results (smooth curves) from Hansen.[4] – × – × curves from conformal solution theory with $\omega_l \neq \omega_s$.

are some discrepancies particularly at the Bi rich end. Since neither Bi nor Sb are simple metals, it is possible that the interaction energy is concentration and temperature dependent. In any case it seems that we need some modification of the conformal solution model (with ωs' independent of T) in this case.

8 MINIMUM TYPE PHASE DIAGRAMS†

Having considered at least briefly types (i), (ii) and (iv) of Figure 1, we turn finally to (v), the minimum-type phase diagram. We have already remarked that no such diagram is possible for ideal solutions. However, it is interesting in this connection to return to the slopes of the liquidus and solidus curves given by Eqs. (3.10) and (3.11). In the alloys considered here, S_{CC} is always finite and it follows therefore that $\Delta T/\Delta c_l$ and $\Delta T/\Delta c_s$ both are zero when $c_l = c_s$, a property characterizing the minimum-type phase diagram (v) of Figure 1. Thus, the possibility of such solutions exists in the present formalism.

We shall return to this point below, but it will be convenient first to consider a specific example Au–Cu. Calculations for the ideal case have been made, and, inevitably, lead to a simple ascending diagram in disagreement with experiment. Using heat of mixing data,[5] we have estimated $\omega_l = -3275\,°\mathrm{K}$ and $\omega_s = -2440$. Immediately a minimum type phase diagram is obtained and without any adjustment of ω_l and ω_s the correct minimum

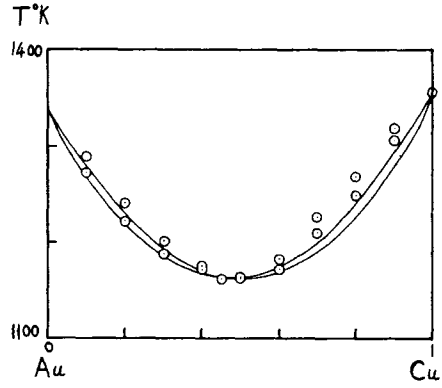

FIGURE 5 Liquidus and solidus curves for Au–Cu. ⊙ Experimental points taken from Hansen.[4] Curves from conformal solution model.

† Our arguments below are about turning points rather than minima. To our knowledge, all binary metallic phase diagrams have turning points which are minima. However, maxima are possible in principle (see comments of Ag–Au).

temperature T_m is predicted. Figure 5 shows the results, and though qualitative differences remain elsewhere in the phase diagram, the agreement between theory and experiment is good.

In fact, it turns out that the minimum temperature T_m and the corresponding concentration c_m depend *entirely* on $\omega_l - \omega_s$ for conformal solutions, *not* on ω_l and ω_s separately, as we shall now demonstrate. Returning to Eqs. (2.9) and (2.10) we see that when $c_l = c_s = c_m$ at $T = T_m$ then

$$\frac{\gamma_A^l}{\gamma_A^s} = \exp\left(-\frac{F_{AO}}{RT_m}\right) \quad \text{and} \quad \frac{\gamma_B^l}{\gamma_B^s} = \exp\left(-\frac{F_{BO}}{RT_m}\right). \tag{8.1}$$

But for conformal solutions, the activity coefficients are given by Eqs. (5.6) and (5.7) and Eqs. (8.1) become

$$e^{(\omega_l-\omega_s)c_m^2/RT_m} = e^{-F_{AO}/RT_m} \tag{8.2}$$

and

$$e^{(\omega_l-\omega_s)(1-c_m)^2/RT_m} = e^{-F_{BO}/RT_m}. \tag{8.3}$$

This demonstrates that in conformal solution theory, when (8.2) and (8.3) have physical solutions for T_m and c_m, they can *only* depend on $\omega_l - \omega_s$. Putting $\omega_l = \omega_s$, it is clear that *no* solutions of minimum type exist.

We have here discussed the turning points as minima. But we want to record here that in the course of our calculations on Ag-Au that we discussed above, the effect of changing ω_s to $-2500°K$ was studied. A *maximum* type diagram resulted, with $T_{max} = 1372°K$. It seems therefore that the pronounced (concave) curvature in the measured liquidus-solidus curves for Ag–Au shown in Figure 2, as compared with the flatter ideal solution curves, could properly be considered as due to a (weak) tendency to form a maximum type diagram. In fact, as remarked earlier in connection with Figure 2, a much *smaller* difference between ω_l and ω_s is required to get a curvature in agreement with experiment.

In the same vein, for Cd–Mg we find for $\omega_s = -2000°K$ a minimum solution, with its minimum at $c_{Mg} \simeq 0.3$. While, in practice, the difference between ω_2 and ω_s is much too small to induce a minimum, the pronounced convex curvature can be thought of as due to a tendency towards a minimum-type diagram in this alloy. The fact that the width of the observed region between solidus and liquidus is wider at the Mg rich end (see Figure 3) is quite consistent with this point of view.

9 DISCUSSION AND SUMMARY

The most important consequence of the thermodynamics of the liquidus and solidus curves given here is that the possibility of minimum-type phase

diagrams is immediately seen to be contained in the theory. However, the limit of ideal solutions loses the minimum-type behaviour, only ascending diagrams being possible. Furthermore, we have demonstrated (see Eqs. (8.2) and (8.3)) that the conformal solution model for both liquid and solid solutions leads to minimum-type behaviour only if $\omega_l \neq \omega_s$.

But for Au–Cu, if we retain the conformal solution model, but estimate ω_l and ω_s from heats of mixing in the liquid and solid state, then we immediately obtain a minimum-type diagram, with a minimum temperature in agreement with experiment. Differences of detail remain, but all the general features are clearly given by the present treatment.

For the ascending type diagrams, departures from ideality are evident now only from quantitative comparisons. The conformal solution model is useful in Cd–Mg, and to a lesser extent in Ag–Au, and Bi–Sb. The indications are that in numerous systems, departures from such a model will have to be incorporated. This is clearly the case, for example, in Au–Pt (see (iii) of Figure 1), where from the shape of the solidus curve[7] the concentration fluctuations in the solid must peak around a Pt concentration of 0.6 and then decrease rapidly by a concentration of 0.7.

Needless to say, the behaviour of S^s_{CC} must reflect the electronic structure of the alloy, filling of Brillouin zones etc. This is a matter for future work, but it is worthwhile to conclude with two remarks related to this point. First of all March, Tosi and Bhatia[7] have demonstrated an intimate connection between S_{CC} and the electron-electron correlation function S_{ee} in highly conducting metallic alloys. Secondly, when conformal solution theory is appropriate, all solution properties can be related to those of a *reference* liquid. In particular, the interaction energy ω can be calculated explicitly from a knowledge of the radial distribution function g(r) and the pair interaction $\phi(r)$ in the reference liquid. For the simpler metallic alloys (e.g. K–Rb, which has a minimum-type phase diagram) the calculation of $\phi(r)$ can again be tackled from electron theory. Thus, the present work, while thermodynamical in origin, can be viewed as representing a further step towards relating phase equilibria to structure, both ionic and electronic.

References

1. A. B. Bhatia and N. H. March, *Phys. Letters* **41A**, 397 (1972).
2. A. B. Bhatia and N. H. March, *J. Phys. F.* **5**, 1100 (1975).
3. A. B. Bhatia and D. E. Thornton, *Phys. Rev.* **B4**, 2325 (1971).
4. M. Hansen, *Constitution of Binary Alloys* (McGraw-Hill, New York, 1958).
5. R. Hultgren, R. L. Orr, P. D. Anderson and K. K. Kelly, *Selected Values of Thermodynamic Properties of Metals and Alloys* (John Wiley and Sons, Inc., New York, 1963).
6. H. C. Longuet-Higgins, *Proc. Roy Soc.* **A205**, 247 (1951).
7. N. H. March, M. P. Tosi and A. B. Bhatia, *J. Phys. Chem.*, **6**, L59 (1973).
8. A. Reisman, *Phase Equilibria* (Academic Press, New York, 1970).
9. J. S. Rowlinson, *Liquids and Liquid Mixtures* (Butterworth & Co., 2nd Ed., 1969).

Appendix

PERTURBATIVE TREATMENT OF DEPARTURES FROM IDEALITY

To assess the effects of small departures from ideality, let us treat the case when both $|\frac{\omega_l}{RT}| \ll 1$ and $|\frac{\omega_s}{RT}| \ll 1$. Then we can write

$$\frac{\gamma_A^l}{\gamma_A^s} \doteq 1 + \frac{\omega_l c_l^{i2}}{RT} - \frac{\omega_s c_s^{i2}}{RT} \tag{A1}$$

where, in the "correction" terms $\alpha\omega$ we have replaced c_l and c_s by their "ideal" values c_l^i and c_s^i. Similarly we can write

$$\frac{\gamma_B^l}{\gamma_B^s} \doteq 1 + \frac{\omega_l}{RT}(1 - c_l^i)^2 - \frac{\omega_s(1 - c_s^i)^2}{RT}. \tag{A2}$$

Then we can evidently express the equilibrium conditions (2.9) and (2.10), if we neglect the specific heat differences Δ in Eqs. (4.4) and (4.5) in the form

$$\frac{1 - c_l}{1 - c_s} = A(T)\left[1 - \frac{\omega_l c_l^{i2}}{RT} + \frac{\omega_s c_s^{i2}}{RT}\right] \tag{A3}$$

and

$$\frac{c_l}{c_s} = B(T)\left[1 - \frac{\omega_l}{RT}(1 - c_l^i)^2 + \frac{\omega_s(1 - c_s^i)^2}{RT}\right], \tag{A4}$$

$A(T)$ and $B(T)$ being defined in Eqs. (5.1) and (5.2). After a short calculation, we can then write c_l, to first order in ω_l and ω_s, in terms of the ideal liquidus $c_l^i(T)$ as

$$c_l(T) = c_l^i(T)\left[1 - \frac{\omega_l - \omega_s}{RT(1 - \frac{B}{A})} + \frac{(A - 1)}{A(1 - \frac{B}{A})^2 RT}\{\omega_l(2B - B^2) - \omega_s\}\right]. \tag{A5}$$

In the special case when not only the interaction is weak in the solid and liquid solutions, but $\omega_l = \omega_s \simeq \omega$ say, then

$$c_l(T) \doteq c_l^i(T)\left[1 + \frac{\omega}{RT}\frac{(1 - A)(B - 1)^2}{A(1 - \frac{B}{A})^2}\right]. \tag{A6}$$

With our convention that $T_{AO} < T_{BO}$, the quantity multiplying ω/RT is always negative and therefore $c_l(T) \geqq c_l^i(T)$ if ω is negative, and $\leqq c_l^i(T)$

if ω is positive. This means that the liquidus curve for small $-$ve ω will always lie *below* the ideal liquidus curve, the opposite situation obtaining for $+$ve ω.

A1 Slopes of solidus and liquidus curves at end points

If we use the result (A6), we can readily see, since $A-1 \to 0$ as $T \to T_{AO}$ that

$$\frac{\Delta c_1}{\Delta T} \to \frac{\Delta c_1^i(T)}{\Delta T}. \tag{A7}$$

Thus, in the case when $\omega_l = \omega_s = \omega$ and $|\frac{\omega}{RT}| \ll 1$, we expect the actual and ideal curves to start out together from the pure end points.

This is a useful conclusion in understanding binary phase diagrams of the kind we are considering here. It tells us that the minimum-type of diagram, which does not occur in an ideal solution (see below) cannot be explained without a substantial departure from simple conformal solution theory, with $\omega_l = \omega_s$.

In general, of course, we must get the slope of the liquidus from the basic equation (3.11). But for the ideal case we can readily show from Eq. (5.4) that

$$\frac{\Delta T}{\Delta c_1}\Big|_{T_{AO}} = \frac{RT_{AO}^2}{L_{AO}} \frac{B(T_{AO})}{1 - B(T_{AO})}. \tag{A8}$$

Since from Eq. (5.2), $B(T_{AO}) < 1$, $\Delta T/\Delta c_1|_{T_{AO}}$ is always positive. This demonstrates that non-ideality is crucial for minimum-type phase diagrams. Even in conformal solutions, as we have seen, minimum-type diagrams can occur only if $\omega_l \neq \omega_s$.